

Electronic Supplementary Information

Stimuli-Responsive Methionine-Based Zwitterionic Methacryloyl Sulfonium Sulfonate Monomer and Corresponding Antifouling Polymer with Tunable Thermosensitivity

Tanmoy Maji, Sanjib Banerjee, Avijit Bose and Tarun K. Mandal*

Polymer Science Unit, Indian Association for the Cultivation of Science, Jadavpur, Kolkata 700
032, India

Contents

	Page No.
Table S1. Effect of Anions and its concentrations....at Different pHs.	S1
Figure S1. ^1H NMR spectrum of Boc-L-Methionine	S2
Figure S2. ESI-MS spectrum of Boc-L-Methionine	S3
Figure S3. ^1H NMR spectrum of METMA	S4
Figure S4. ^{13}C NMR spectrum of METMA	S5
Figure S5. ESI-MS spectrum of METMA	S6
Figure S6. ^1H NMR spectrum of METMASPS	S7
Figure S7. ^{13}C NMR spectrum METMASPS	S8
Figure S8. ESI-MS spectrum of METMASPS	S9
Figure S9. FTIR spectra of (a) METMA (b) METMASPS and (c) PMETMASPS	S10
Figure S10. ^1H NMR spectrum of PMETMASPS	S11
Figure S11. SEC traces of (a) PMETMASPS ₁₀₀ ,water with 0.1 M LiBr	S12
Figure S12. (A) Turbidity curves ...METMASPS... pH of the solution	S12
Figure S13. Zeta potentials of of 1.0 wt % aqueous.....at different pHs at 25 °C.	S13
Figure S14. Turbidity curves of PMETMASPS ₅₀(A) SO ₄ ²⁻ and (B) H ₂ PO ₄ ⁻	S13
Figure S15. Turbidity curves of PMETMASPS ₅₀(A) Ct ³⁻ and (B) Ac ⁻ .	S14
Figure S16. Variation of hydrodynamic diameters.....by DLS at 25 °C	S14
Figure S17. Variation of hydrodynamic diameters.....by DLS measurement	S15
Figure S18. Turbidity curves of PMETMASPS ₇₅with varying cations	S15
Figure S19. Turbidity curves of zwitterionic PMETMASPS ₅₀ at different pHs.	S16
Figure S20. MALDI-TOF-MS spectrum of PNIPAM	S16

Table S1. Effect of anions and its concentrations on the phase behaviour of aqueous PMETMASPS₅₀ solution (1 wt%) at different pHs.

pH	Anions	CSC ([M])		Concentration ([M])	Cloud point (T_{cp}) (°C)
		Transmittance Study	DLS Study		
3.5	SO ₄ ²⁻	0.45	0.45	0.45	13.0
				0.50	25.4
				0.55	35.0
				0.65	53.4
				0.72	66.6
	H ₂ PO ₄	0.50	0.50	0.50	13.5
				0.65	37.0
				0.80	61.5
8.0	Ct ³⁻	0.27	0.27	0.27	18.8
				0.30	35.8
				0.34	50.7
				0.37	66.6
	Ac ⁻	2.3	2.25	2.30	17.2
				2.55	40.1
				2.80	64.4
	SO ₄ ²⁻	0.38	0.36	0.38	16.7
				0.45	43.4
				0.48	55.1
				0.53	68.2

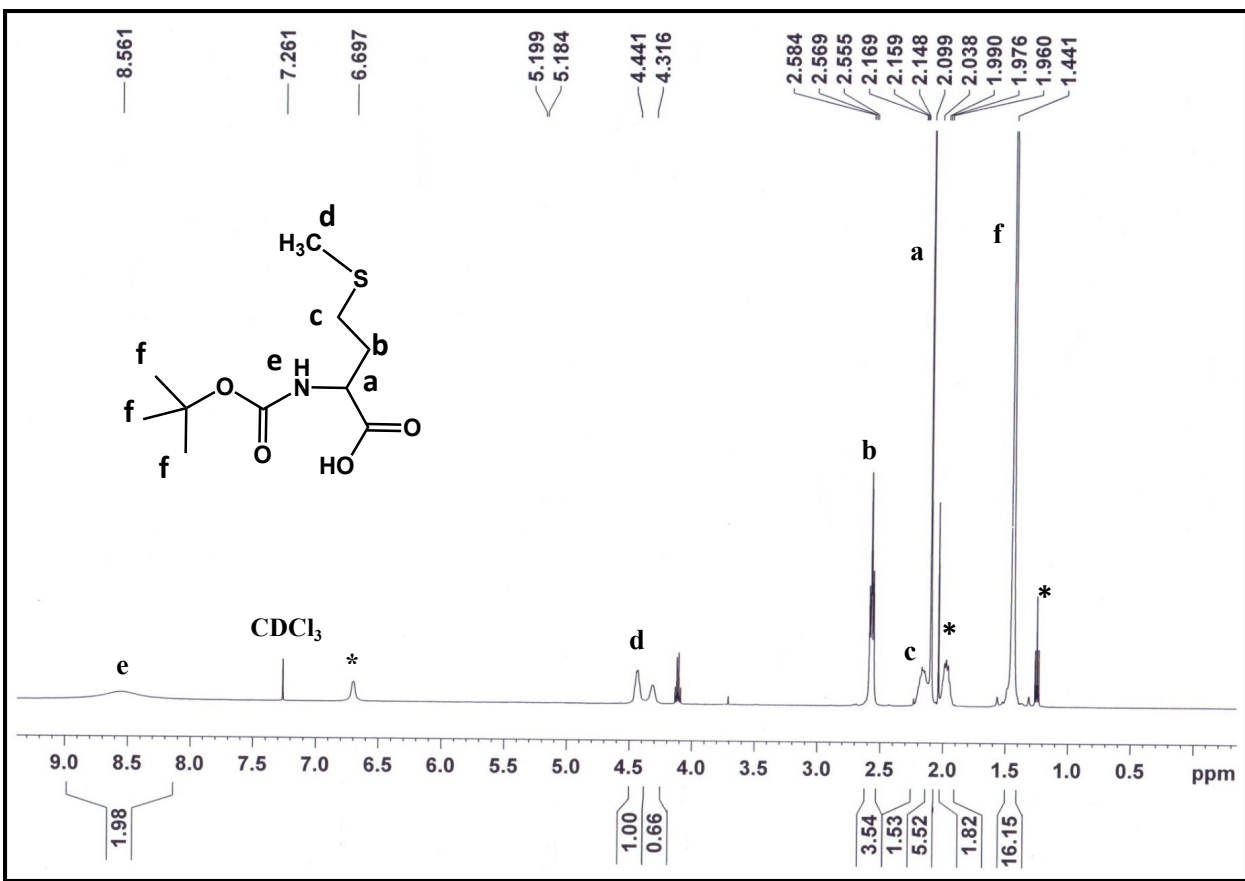


Figure S1. ^1H NMR spectrum of Boc-L-Methionine (Signal at δ 7.2 ppm corresponds to CHCl₃ present in CDCl₃).

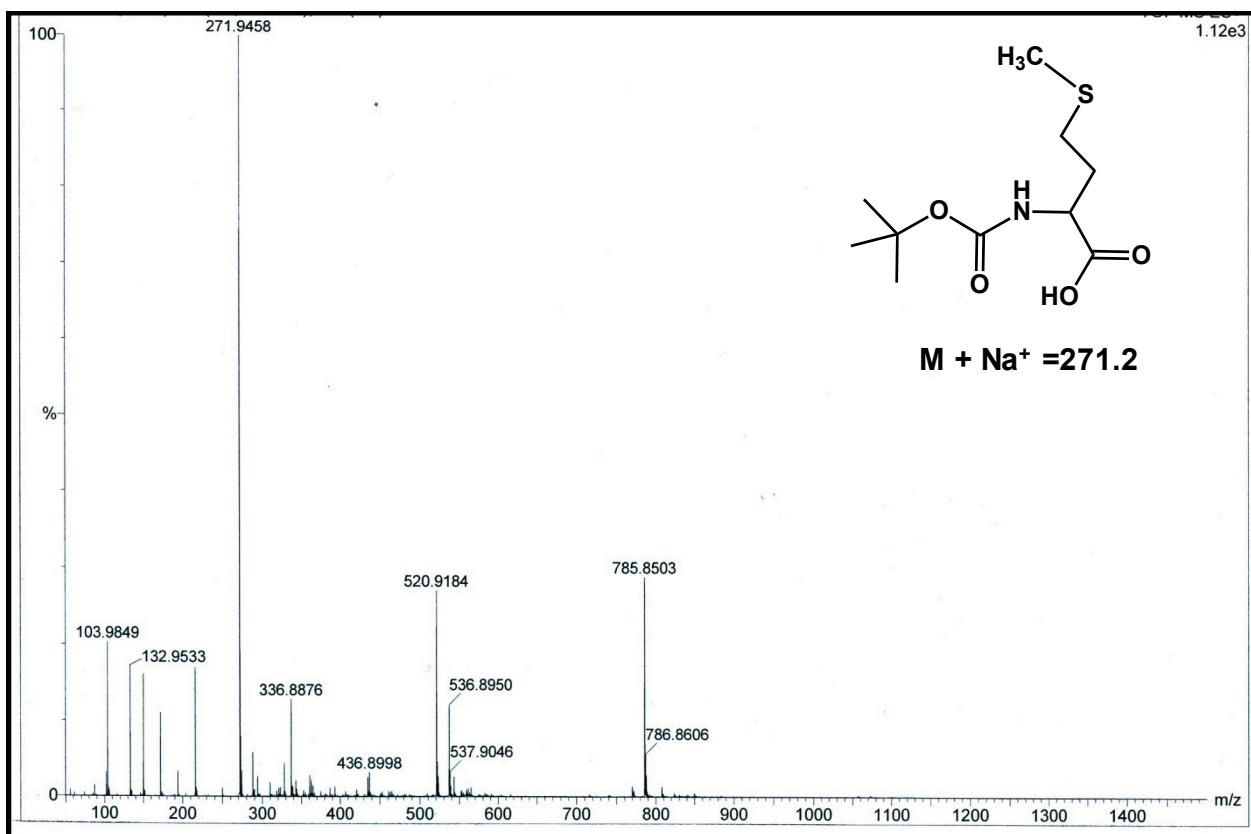


Figure S2. ESI-MS spectrum of Boc-Meth-OH ($M/z + H^+ = 271.2$).

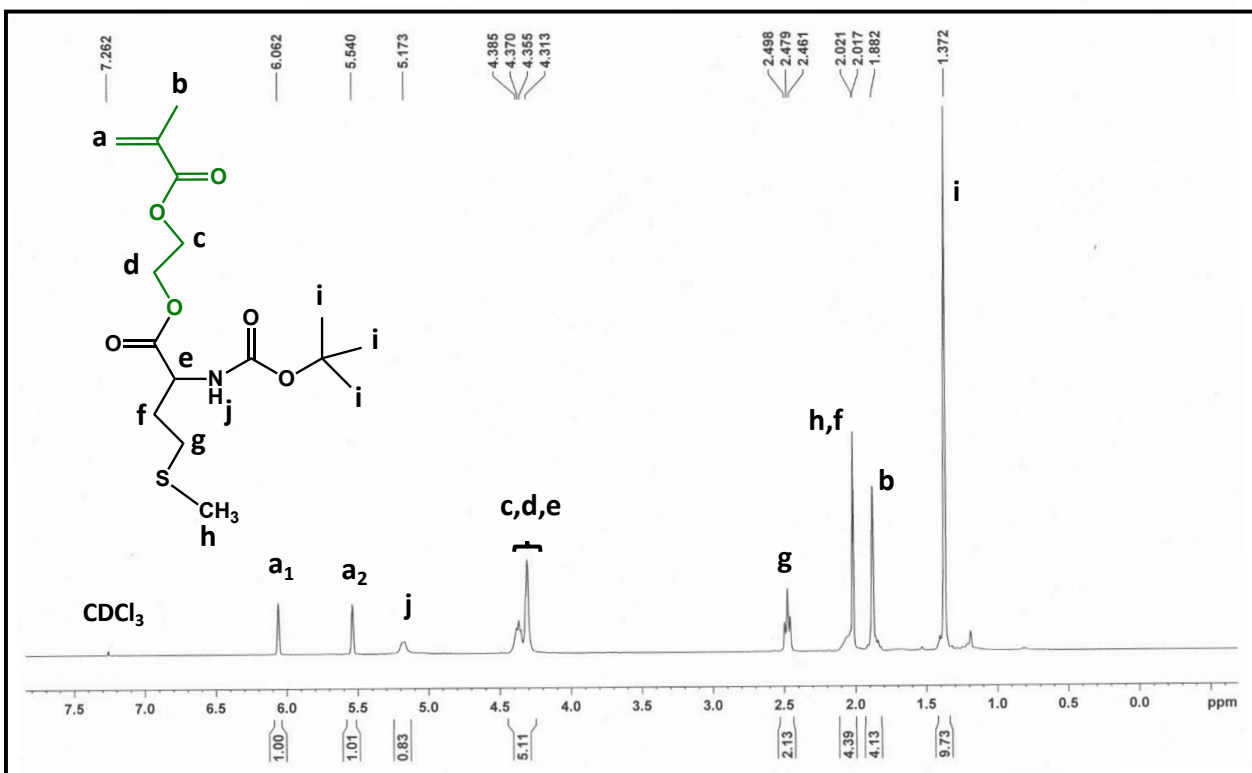


Figure S3. ^1H NMR spectrum of Boc-L-methionine-(2-methacryloylethyl)ester (Signal at δ 7.2 ppm corresponds to CHCl_3 present in CDCl_3).

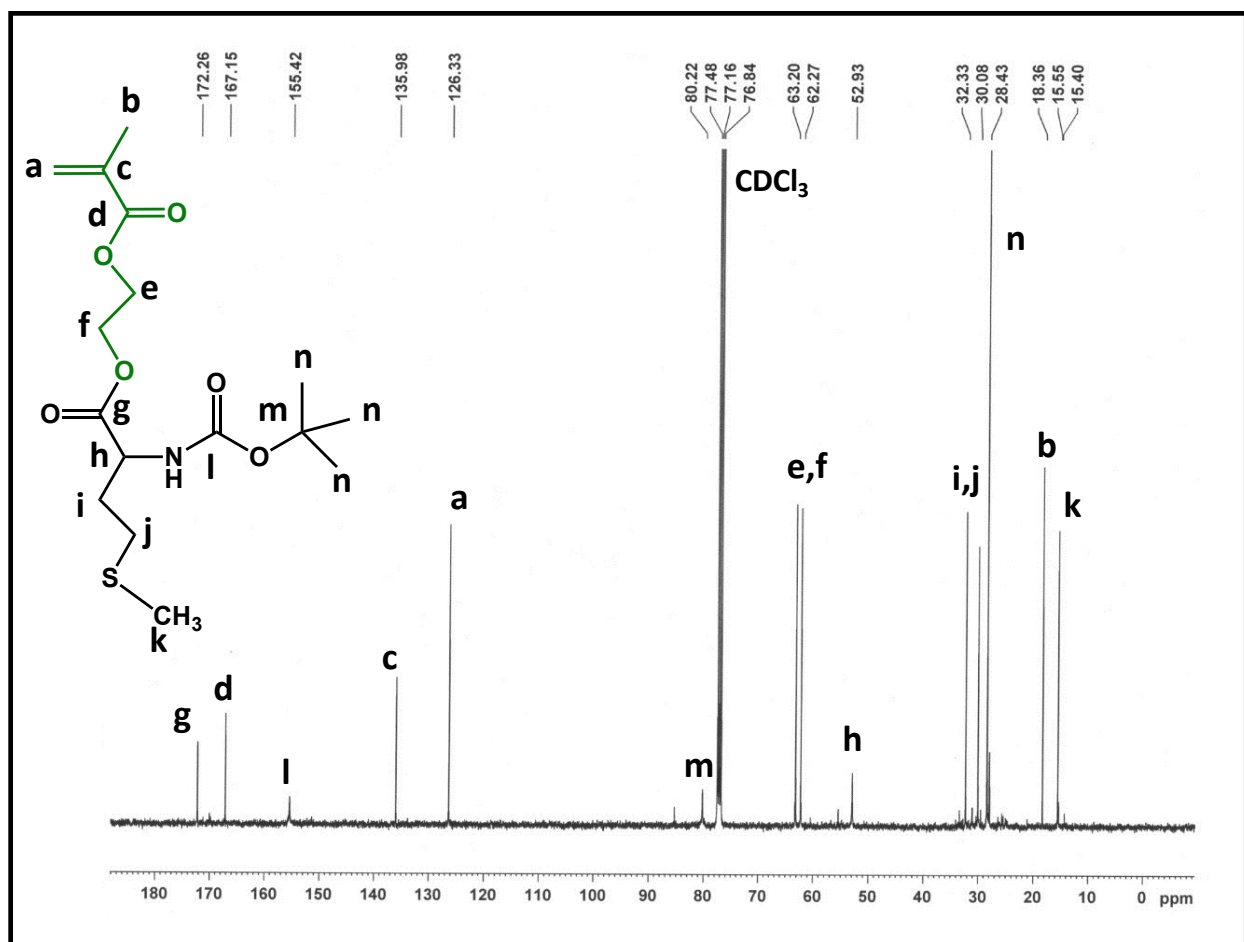


Figure S4. ^{13}C NMR spectrum of Boc-L-methionine-(2-methacryloyloethyl)ester

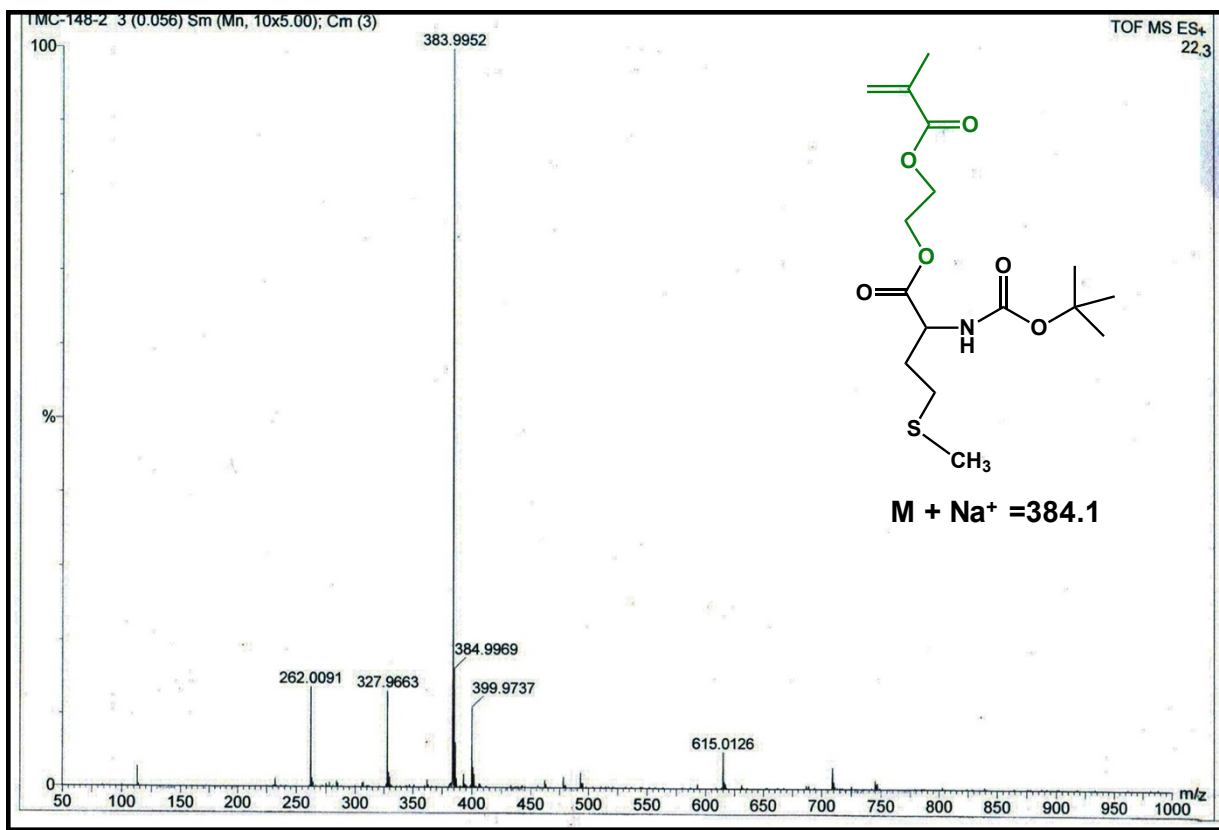


Figure S5. ESI-MS spectrum of Boc-L-methionine-(2-methacryloylethyl)ester ($M/z + Na^+ = 384.1$).

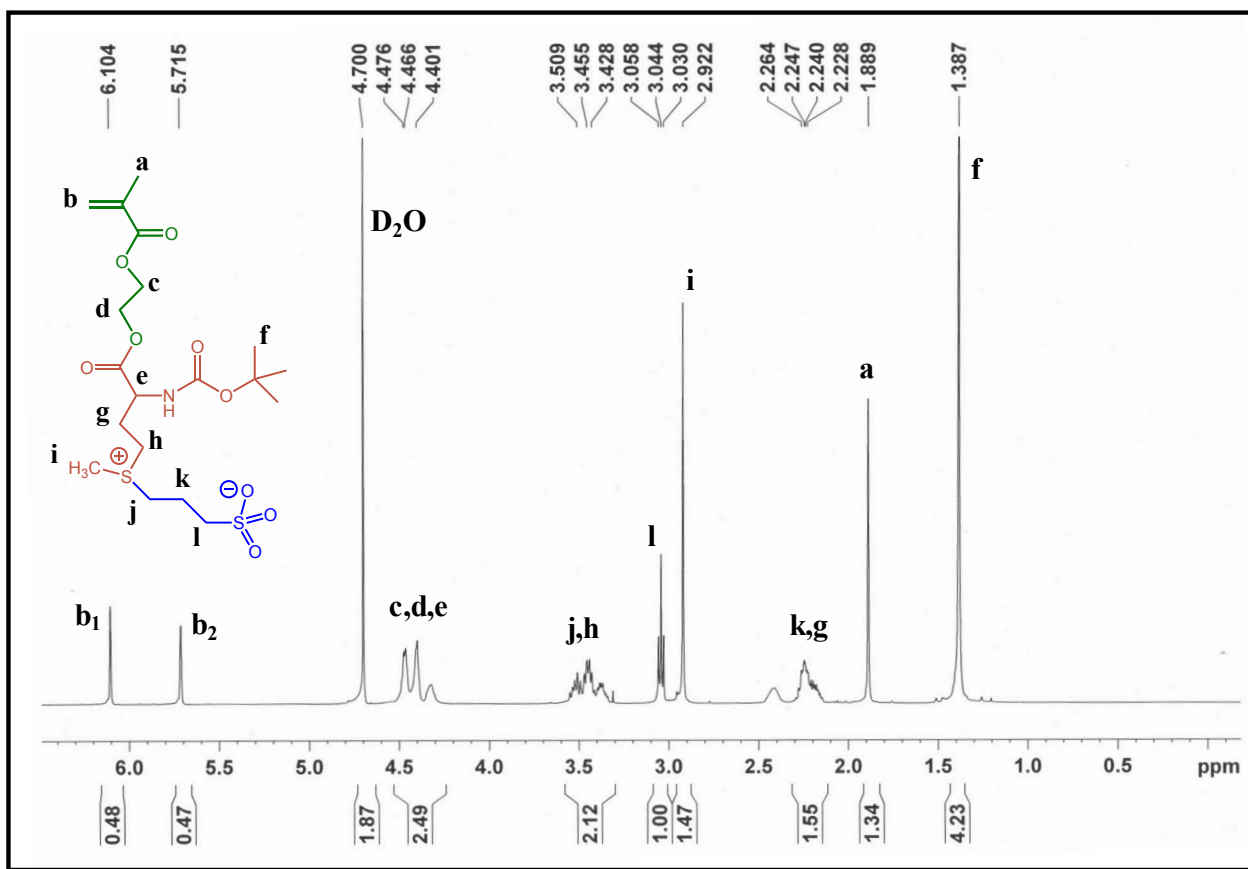


Figure S6. ^1H NMR spectrum of METMASPS (The ^1H NMR 500 MHz, D_2O , signal at δ 4.7 ppm corresponds to water present in D_2O).

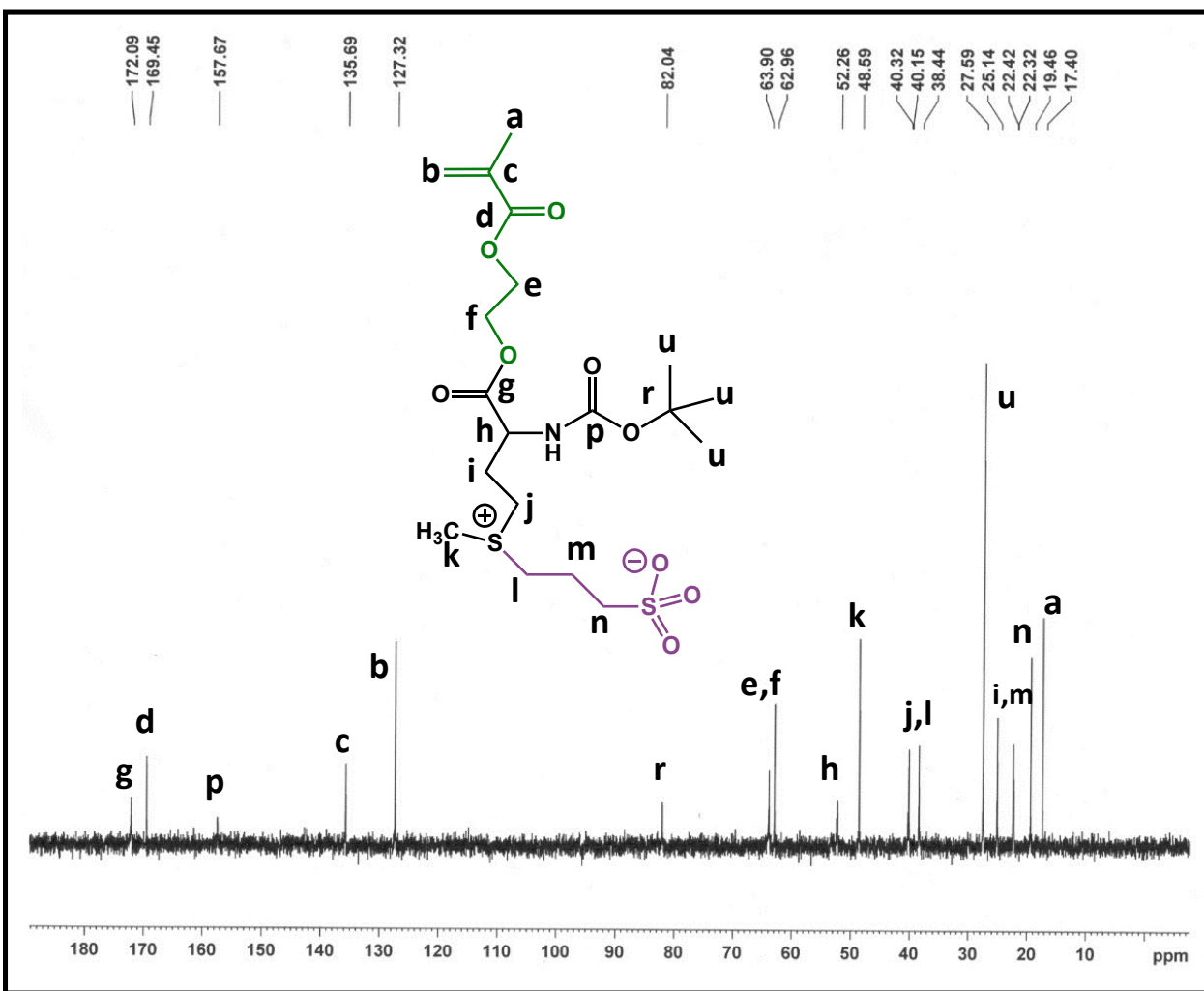


Figure S7. ^{13}C NMR spectrum of METMASPS (^{13}C NMR 500 MHz, D_2O).

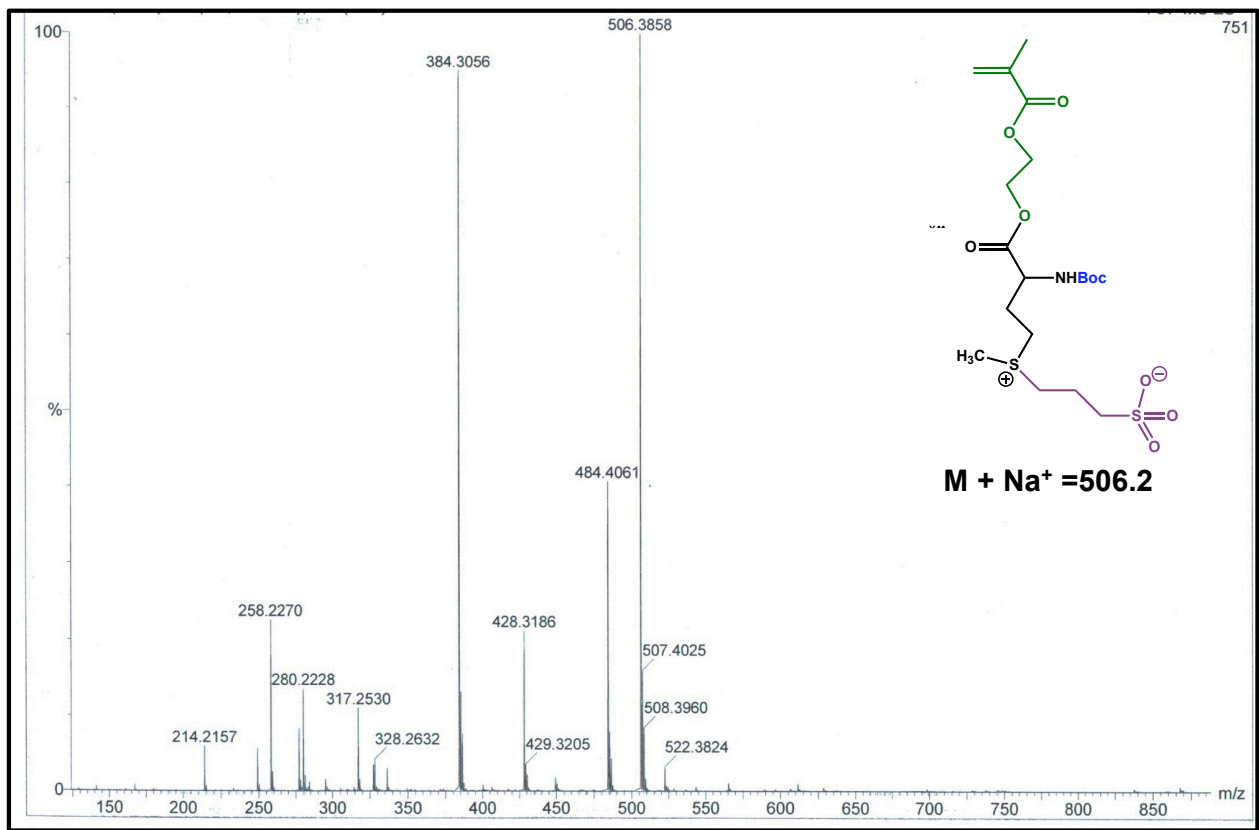


Figure S8. ESI-MS spectrum of METMASPS ($M/z + Na^+ = 506.2$).

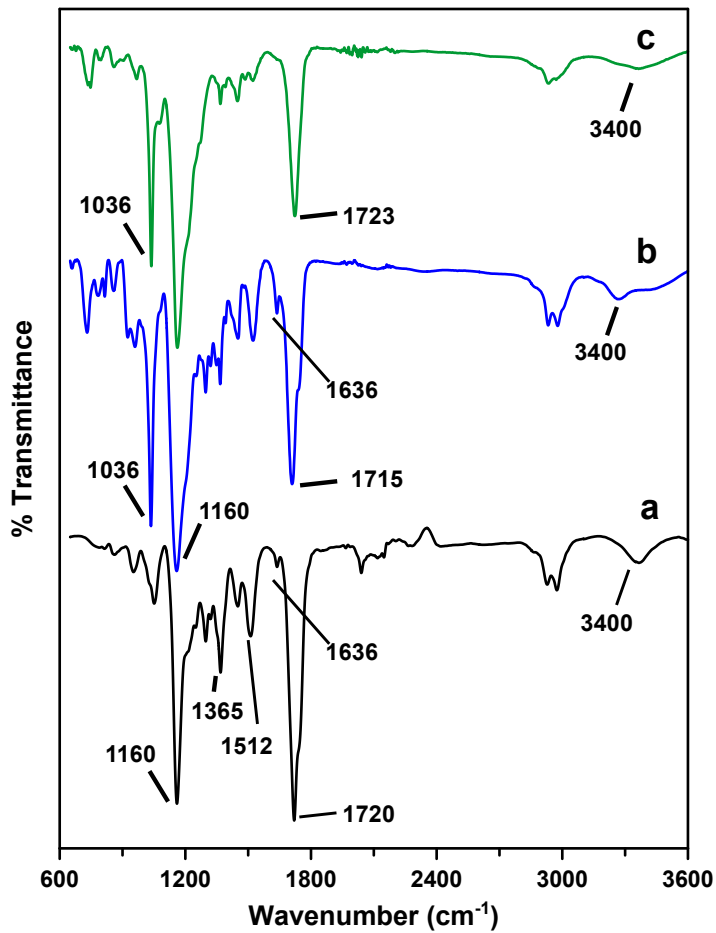


Figure S9. FTIR spectra of (a) METMA (b) METMASPS and (c) PMETMASPS acquired in ATR mood.

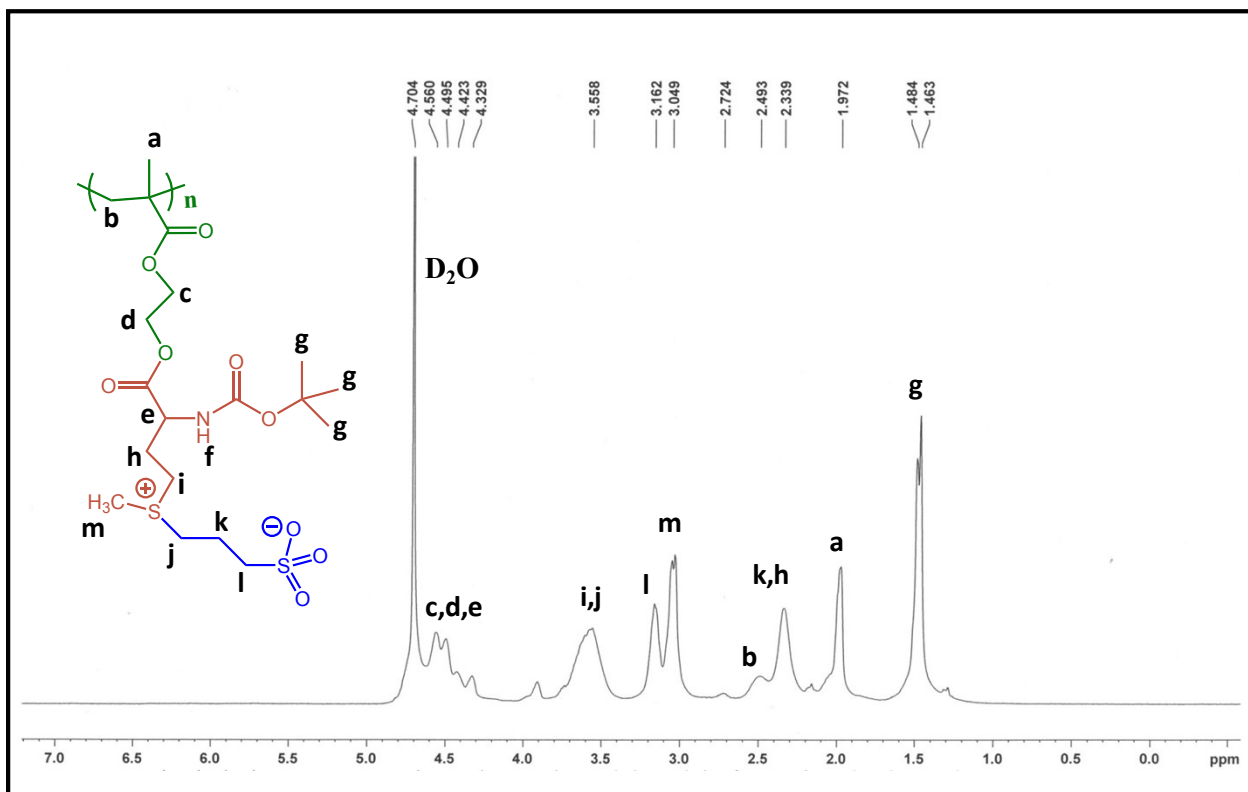


Figure S10. ^1H NMR spectrum of PMETMASPS (The ^1H NMR 500 MHz, D_2O , signal at δ 4.7 ppm corresponds to water present in D_2O).

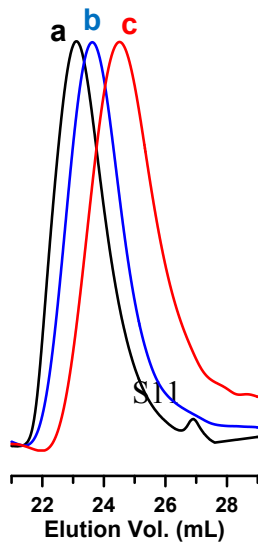


Figure S11. SEC traces of (a) PMETMASPS₁₀₀, (b) PMETMASPS₇₅, and (c) PMETMASPS₅₀ samples (Table 1). Eluent for SEC was water with 0.1 M LiBr.

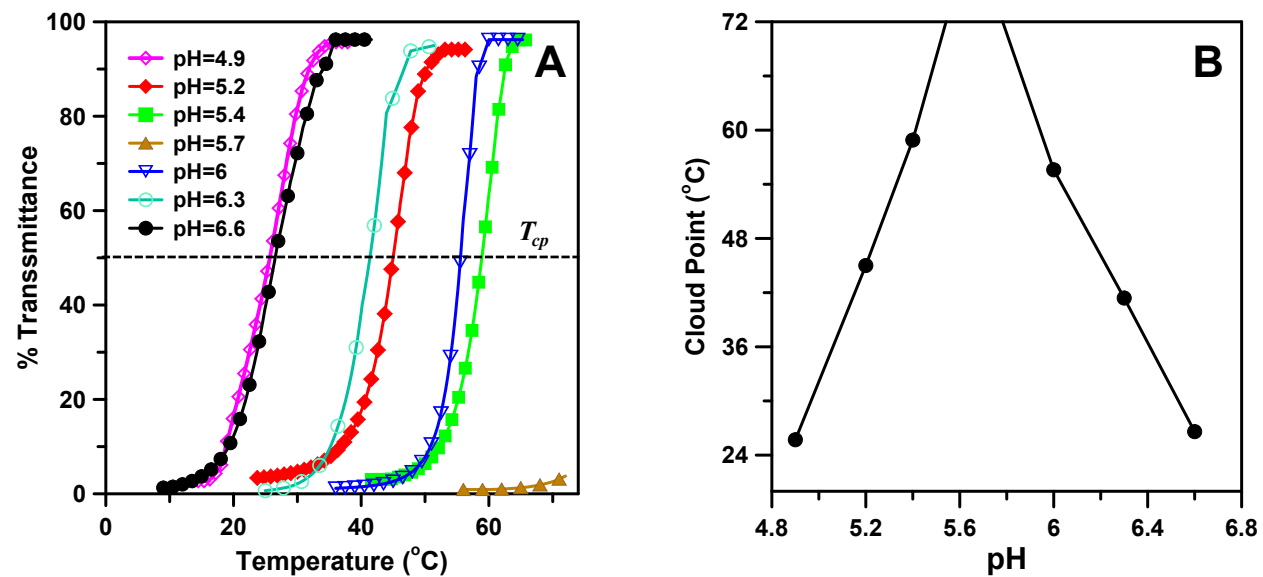


Figure S12. (A) Turbidity curves for the aqueous METMASPS monomer solution (1 wt%) at different pHs. (B) The plot of cloud point of the aqueous METMASPS solution (1 wt%) against pH of the solution.

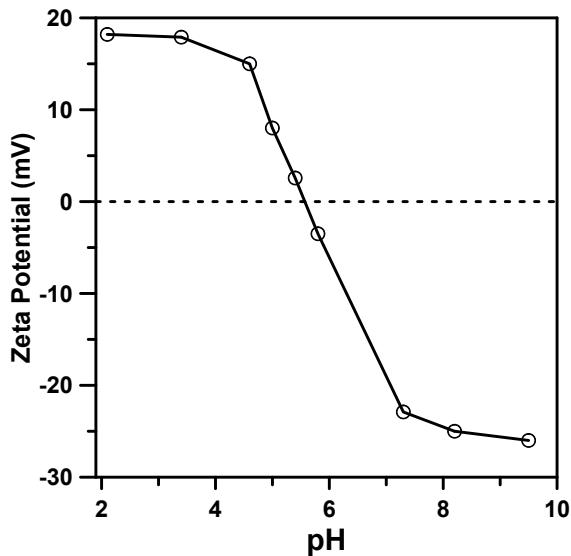


Figure S13. Zeta potentials of of 1.0 wt % aqueous solution of PMETMASPS at different pHs at 25 °C.

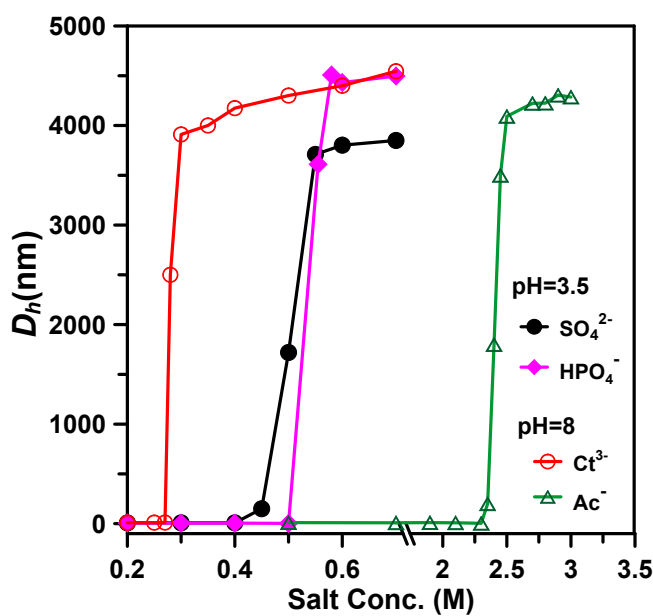


Figure S14. Variation of hydrodynamic diameters (measured by DLS) of 1.0 wt % aqueous solution of PMETMASPS₅₀ with increasing different anions concentration at 25 °C.

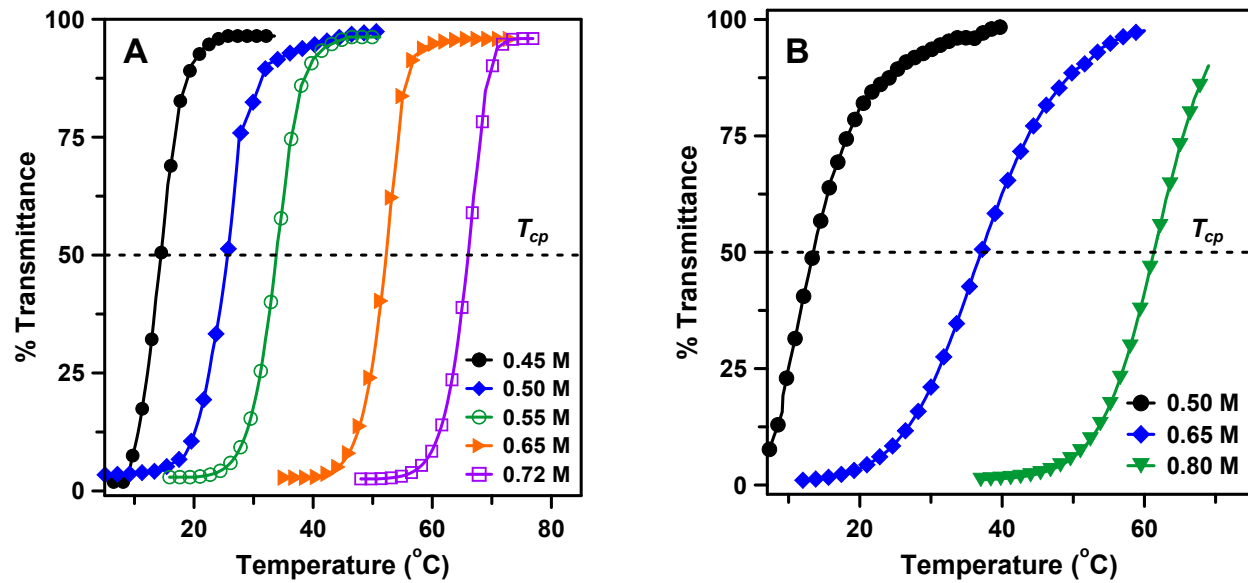


Figure S15. Turbidity curves (at $\lambda = 600$ nm) of zwitterionic PMETMASPS₅₀ (0.1 wt %) in water in presence of different concentration of (A) SO_4^{2-} and (B) H_2PO_4^- anions.

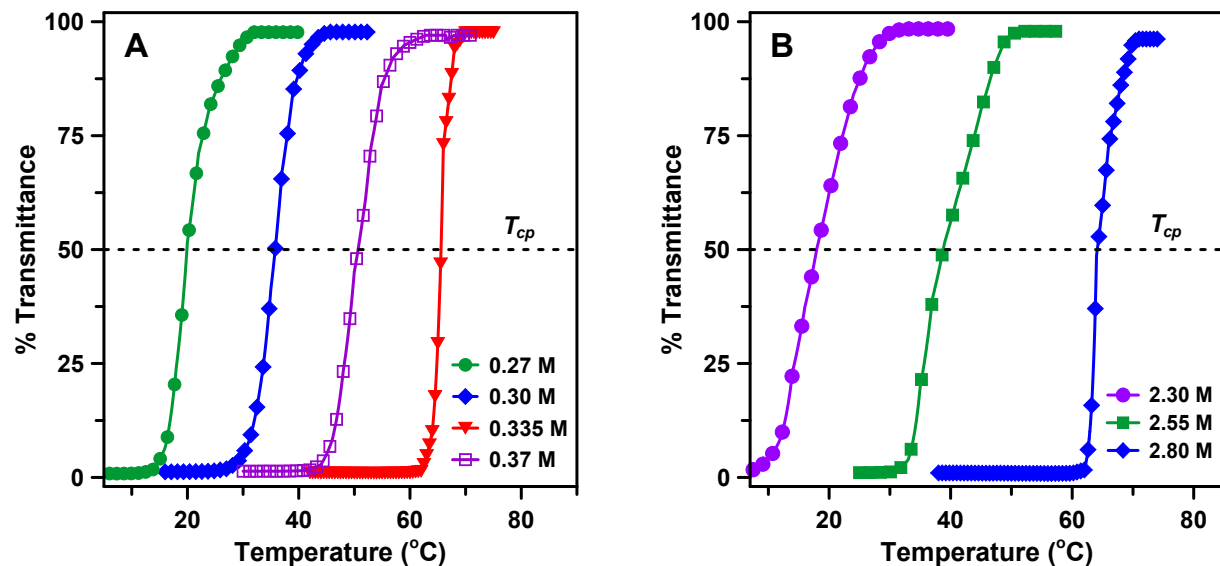


Figure S16. Turbidity curves (at $\lambda = 600$ nm) of zwitterionic PMETMASPS₅₀ (0.1 wt %) in water in presence of different concentration of (A) Ct³⁻ and (B) Ac⁻ anions.

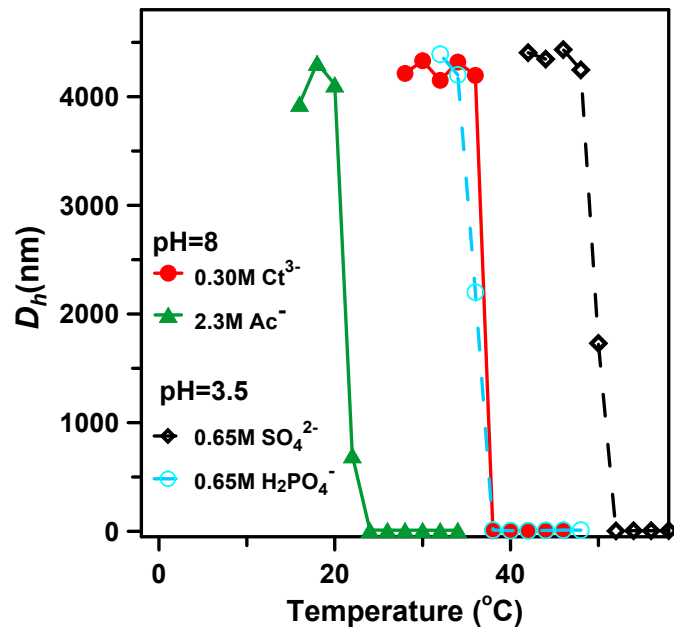


Figure S17. Variation of hydrodynamic diameters (measured by DLS) of 1.0 wt % aqueous solution of PMETMASPS₅₀ with increasing temperature in presence of different kosmotropic anions.

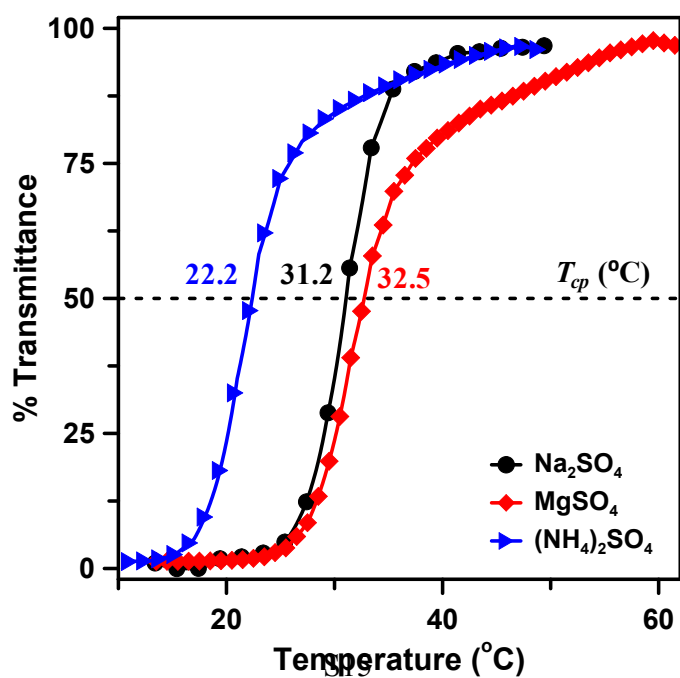


Figure S18. Turbidity curves (at $\lambda = 600$ nm) of aqueous 1 wt % zwitterionic PMETMASPS₇₅ in presence of 0.5M SO₄²⁻ ion from various salts at pH 3.5.

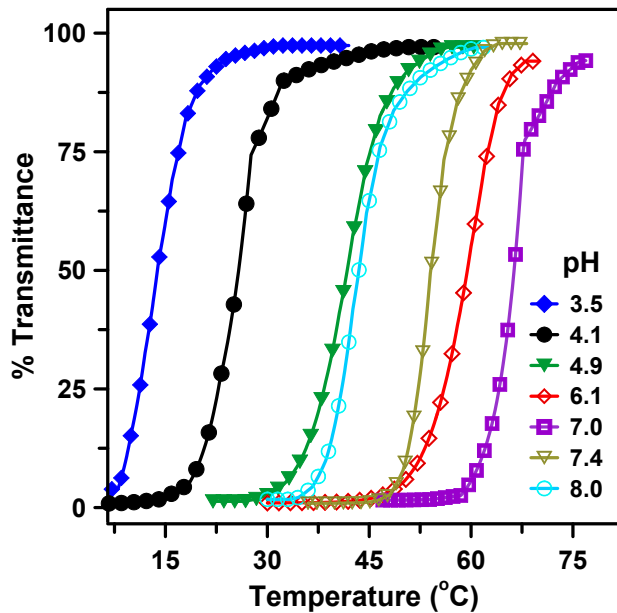


Figure S19. Turbidity curves (at $\lambda = 600$ nm) of zwitterionic PMETMASPS₅₀ (0.1 wt %) in water in presence of 0.45 M SO₄²⁻ at different pHs.

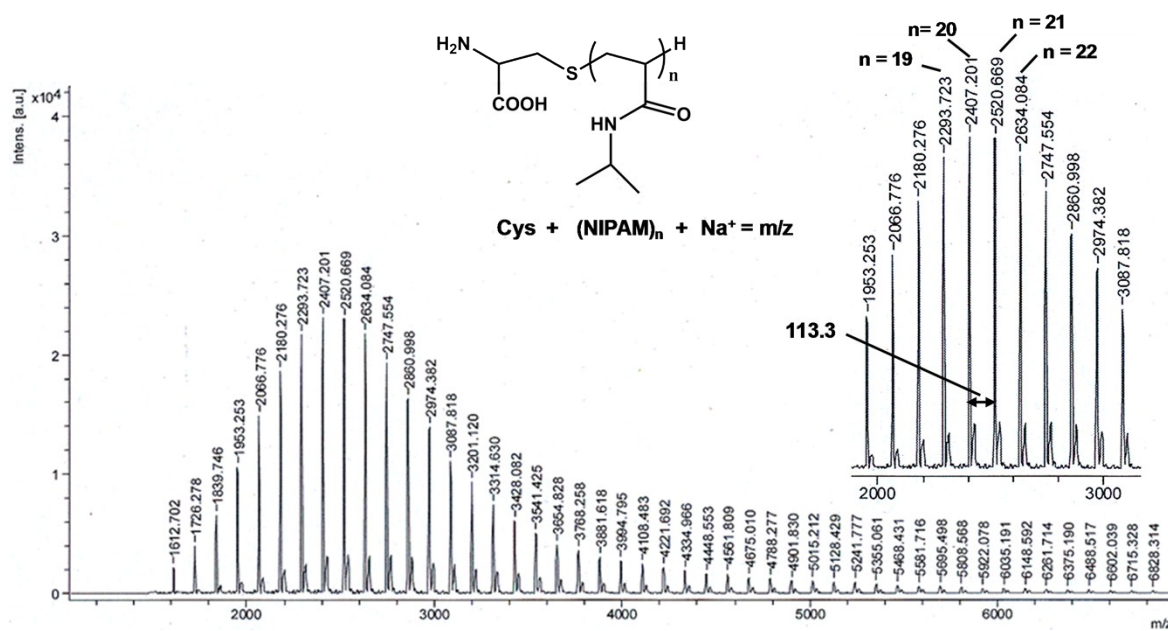


Figure S20. MALDI-TOF-MS spectrum of PNIPAM.